Forest Chemicals Review
www.forestchemicalsreview.com
ISSN: 1520-0191
March-April 2022 Page No. 877-894
Article History: Received: 08 February 2022, Revised: 10 March 2022, Accepted: 02 April 2022, Publication: 30 April 2022

Wireless Charging Control Strategy of Electric Vehicle Using Compensating Network

Yaya Wang* and Yajuan Jia
Xi`an Traffic Engineering Institute, Meibei Xi Lu, Binhe New District, Xi 'an District, Shaanxi Province, xi'an, 710300, China
*Corresponding Author.

Abstract:

This thesis aims to increase the charging distance and improve the charging efficiency of electric vehicles. The wireless charging control strategy of electric vehicles is studied by using the principle of magneto-fluid mechanics and magnetic resonance coupling wireless power transfer (MRC-WPT) system. First, the calculation method of coil parameters of four-coil MRC-WPT system is proposed, and the transmission characteristics of four-coil MRC-WPT system are analyzed, including the output voltage gain, input current gain, output power and transmission efficiency of traditional Serial-Serial-Serial-Serial (SSSS) compensating network. Then, Inductor-Capacitor-Capacitor (LCC) compensating network is introduced into the driving coil side to form a four-coil MRC-WPT structure of Inductor-Capacitor-Capacitor-Serial-Serial-Serial (LCC-SSS) compensating network. Then, the formed network is analyzed. The experimental platform is built to collect the input voltage, output voltage and other data of the system under the SSSS compensating network and LCC-SSS compensating network when the output voltage of the driving coil is 50V and the inductance coefficient is 0.5. The results reveal that when the inductance coefficient is 0.5, the maximum output power of LCC-SSS compensating network can reach 85W, while that of SSSS compensating network is only 10W. This is because there are no energy consuming components in the wireless charging system based on LCC-SSS compensation network. Through the combination of passive components, the energy in the system is stored in the resonant element without input series resistance, which increases the voltage acting on the driving coil, increases the input current flowing through the system, and improves the output power of the system. Finally, the curve is drawn to verify that the MRC-WPT system based on LCC-SSS compensating network can effectively improve the scientificity and feasibility of system transmission efficiency. This thesis has certain reference significance for the compensating network optimization of electric vehicle wireless charging system.

Keywords*: Magneto-fluid mechanics; magnetic coupling resonance; wireless transmission system; compensating network; electric vehicle.*

I. INTRODUCTION

Under the background of global warming, energy crisis and air pollution, traditional motor vehicles urgently need transformation because of their defects, such as high pollution and high emission, while

Forest Chemicals Review
www.forestchemicalsreview.com
ISSN: 1520-0191
March-April 2022 Page No. 877-894
Article History: Received: 08 February 2022, Revised: 10 March 2022, Accepted: 02 April 2022, Publication: 30 April 2022

electric vehicles have attracted much attention because of using clean energy. However, at present, the problem of electric vehicle charging has not been well solved. First, the number of electric vehicle charging piles in cities is limited, and the charging of electric vehicles is far less convenient than that of fuel vehicles. Besides, the charging time is long. The DC charging pile charges fast, but the cost is high. The AC charging pile costs low, but the charging time needs at least 6 hours. Moreover, at present, most charging piles are limited charging, which is not convenient and flexible enough and there is a risk of leakage. A few charging piles are wireless charging, but the transmission efficiency is relatively low [1]. People cannot find ideal solutions to the two technical difficulties of charging and energy storage, so electric vehicles still cannot shake the market position of traditional motor vehicles [2]. With the deepening of magneto-fluid mechanics research, wireless transmission technology has also been developed accordingly. This technology has been applied to aerospace, industry, transportation, and other fields with its safety, reliability, and convenience advantages. Magneto-fluid mechanics is a subject that combines classical fluid mechanics and electrodynamics to study the interaction between conductive fluid and magnetic fields. It includes magnetohydrostatics and magnetohydrodynamics. The basic idea is that the magnetic field can induce current in the moving conductive fluid, and the radio energy transmission technology is studied through this idea. The common wireless transmission modes mainly include magnetic induction, magnetic coupling resonance, microwave, and laser. The working frequency of microwave and laser mode is generally quite high, which is suitable for long-distance wireless transmission, but it has the problem of difficult control. Therefore, magnetic induction and magnetic coupling resonance wireless transmission modes are often used in daily life [3, 4].

The current electric vehicle wireless charging technology is to use magnetic induction to charge the electric vehicle battery, and its charging efficiency can reach more than 96%. The application of this technology in charging electric vehicles close to each other is relatively mature [5]. However, if the charging distance increases, the wireless charging technology of magnetic induction will no longer be applicable. Seo (2019) analyzed the traditional double coil magnetic resonance coupling wireless power transfer (MRC-WPT) system. The system parameters such as the quality factor and coupling coefficient of the resonator lead to the problem of short power transmission distance. Three-coil wireless power transfer (WPT) system is adopted, and the coupling coefficient between transmitting coil and receiving coil should be zero as far as possible to improve power transmission efficiency and transmission distance. The experimental results show that when the coupling coefficient exceeds the critical coupling coefficient, the double coil WPT system has two splitting frequencies far away from the working frequency. In the three-coil WPT system, there will be three splitting frequencies far away from the working frequency, and the splitting frequency in the middle of the three splitting frequencies is not different from the natural resonant frequency of the system [6]. Liao et al. (2019) analyzed the frequency splitting phenomenon of the four-coil MRC-WPT system and gave the mathematical and physical explanation of the frequency splitting phenomenon, and the boundary conditions and frequency division points of frequency splitting. Besides, the amplitude-frequency and phase-frequency characteristics of input impedance were described, and a solution that could help improve the transmission efficiency of the system during frequency splitting was proposed. However, reducing the source resistance in the actual system will also introduce the resistive load. The resistive load will produce additional loss during operation, resulting in low efficiency of the

Forest Chemicals Review
www.forestchemicalsreview.com
ISSN: 1520-0191
March-April 2022 Page No. 877-894
Article History: Received: 08 February 2022, Revised: 10 March 2022, Accepted: 02 April 2022, Publication: 30 April 2022

system [7]. This thesis improves the traditional four-coil MRC-WPT system through the original new method. By increasing the working frequency of the system and designing an appropriate compensation network, the long-distance transmission of radio energy can be realized.

The research purpose is to improve the charging distance of electric vehicles. The research object is electric vehicles' dynamic wireless charging technology based on magnetic coupling resonance. First, the coil parameter calculation method of the four-coil MRC-WPT system is proposed. The transmission characteristics of the four-coil MRC-WPT system are analyzed, and the output voltage gain, input current gain, output power and transmission efficiency of the traditional Serial-Serial-Serial-Serial (SSSS) compensating network are calculated. Then, the Inductor-Capacitor-Capacitor (LCC) compensating network is introduced into the driving coil side to form a four-coil MRC-WPT structure of LCC-Serial-Serial-Serial (LCC-SSS) compensating network. Next, the system is analyzed and calculated. Then, the system's input voltage and output voltage under the SSSS compensating network and LCC-SSS compensating network are collected through experiments. Finally, the curve is drawn to prove that the MRC-WPT system based on the LCC-SSS compensating network can improve system transmission efficiency significantly.

This thesis is to theoretically analyze the advantages of the compensation network, improve the system's output power and transmission efficiency, and provide a certain basis for the optimal design of the compensation network of the four-coil MRC-WPT system. It has certain reference significance for the optimization of wireless charging control strategy for electric vehicles.

II. FOUR-COIL MRC-WPT BASED ON LCC-SSS COMPENSATING NETWORK

2.1 Four-coil MRC-WPT

The four-coil MRC-WPT system is composed of a DC power supply, Radio Frequency Power Amplifier (RFPA), matching circuit, four-coil system and radio frequency load [8]. The four-coil system consists of the driving coil, transmitting relay coil, receiving relay coil and load coil. The function of an RFPA is to change the DC power supply into a high-frequency AC power supply for power supply. The four-coil structure generates high-frequency AC on the load coil through high-frequency magnetic coupling resonance to realize the power supply function for RF load [9, 10].

When the four-coil MRC-WPT system works, the coil inductance and capacitance resonate, and the coils are coupled with each other. The driving coil and the load coil are single turn coils wound by copper wires, and the single turn coil resonates with the compensation capacitance set in the circuit. The transmitting and receiving relay coils are spiral coils wound by Litz wires. The relay coil has a high-quality factor Q. Due to stray capacitance between lines, the coil inductance and stray capacitance resonate during high-frequency operation [11, 12].

In the four-coil MRC-WPT system, the function of the transmitting coil is to resonate the high-

Forest Chemicals Review
www.forestchemicalsreview.com
ISSN: 1520-0191
March-April 2022 Page No. 877-894
Article History: Received: 08 February 2022, Revised: 10 March 2022, Accepted: 02 April 2022, Publication: 30 April 2022

frequency AC power supply output by RFPA and generate a high-frequency magnetic field on the coil. The relay coil stores and relays the energy in the high-frequency magnetic field of the driving coil, and then transmits the energy through the coil. The load coil is responsible for receiving the energy on the relay coil [13]. The relay coil is composed of multiple rings. When the resonant frequencies among the coils are consistent, it can amplify the high-frequency current generated by the transmitting coil.

The RFPA on the transmitting side is connected to the compensating network of the driving coil, and its working frequency is basically the same as the resonant frequency of the whole system. When the driving coil is connected in series with the compensation capacitor, the inductance and capacitor resonate in series, and the energy stored in the coil is transmitted to the next stage through resonance. Then, resonance transmission is carried out through the relay coil to transmit energy to the load coil to supply power to the load [14].

The relay coil consists of a spiral coil. The spiral coil is mainly composed of the plane spiral coil and solenoid coil. The solenoid coil structure is a non-closed ring with the same outer diameter. Its expression reads:

$$L=\mu_0 N^2 r\left[\ln\left(\frac{8r}{a}\right)-\ln N-\frac{1}{2}\right] \quad (1)$$

The inductance of solenoid coil winding is relatively large, the mutual inductance between coils is also relatively large, and the transmission distance is far. In (1), μ_0 is the air permeability and its value is 4π*10-7N/A2. N is the number of turns of the coil. r is the coil radius and a is the wire diameter of the coil conductor [15].

Compared with the solenoid coil structure, the plane solenoid coil structure has a small longitudinal space, suitable for occasions with certain requirements for the coil spatial structure [16]. The inductance calculation reads:

$$L=2\mu_0 N^2 r'\left[\ln\left(\frac{8r'+4Na}{Na}\right)-\frac{1}{2}\right] \quad (2)$$

In (2), r' is the average radius of the plane spiral coil. The distance between the lines of the plane spiral coil is small, and the stray capacitance is relatively large. The expression of its distributed capacitance reads:

$$C_c=\frac{\pi^2\varepsilon_0\varepsilon_r(D_0-N\cdot s+s)}{\cosh^{-1}(s/w)} \quad (3)$$

In (3), w is the diameter of the coil conductor. ε_0 is the vacuum dielectric constant, which is 8.85*10-12F/m. ε_r is the dielectric constant of copper, $\cosh^{-1}(x)=\ln\left(x+\sqrt{x^2-1}\right)$. The working environment of the overall system is at high frequency, and the skin effect causes the current flowing through the conductor to be only a part of the conductor surface [17]. The relay coil is wound with multi-strand Litz wires to reduce the adverse effect of skin effect. The expression of parasitic resistance reads:

Forest Chemicals Review
www.forestchemicalsreview.com
ISSN: 1520-0191
March-April 2022 Page No. 877-894
Article History: Received: 08 February 2022, Revised: 10 March 2022, Accepted: 02 April 2022, Publication: 30 April 2022

$$R_c=\frac{4\rho_{Cu}N(D_0-N\cdot s+s)}{w\delta_{Cu}} \tag{4}$$

In (4), δ_{Cu} represents the skin depth of copper and $\delta_{Cu}(f)=0.066/f_{1/2}$. ρ_C is the conductivity of copper.

In the wireless transmission system, a resonant circuit with high-quality factor is required to make the system work effectively, effectively reducing the useless power in the line, reducing the sensitivity of the system to parameters, and improving the system's stability [18]. Since the inductance of the driving coil and the load coil is small, an external compensation capacitor is needed to make the relay coil have a high-quality factor. The expression of quality factor Q reads:

$$Q=\frac{\omega L}{R} \tag{5}$$

L is the inductance on the circuit, R is the resistance, and ω is the impressed frequency. Equation (5) shows that the quality factor Q of the relay coil can be increased by increasing the coil's inductance, increasing the number of turns of the coil, or reducing the stray capacitance between lines to improve the system's stability.

2.2 Analysis of traditional SSSS compensating network

The driving coil and the load coil resonate with the compensation capacitance set by the circuit. At present, the common connection methods are series. Figure 1 shows its equivalent circuit:

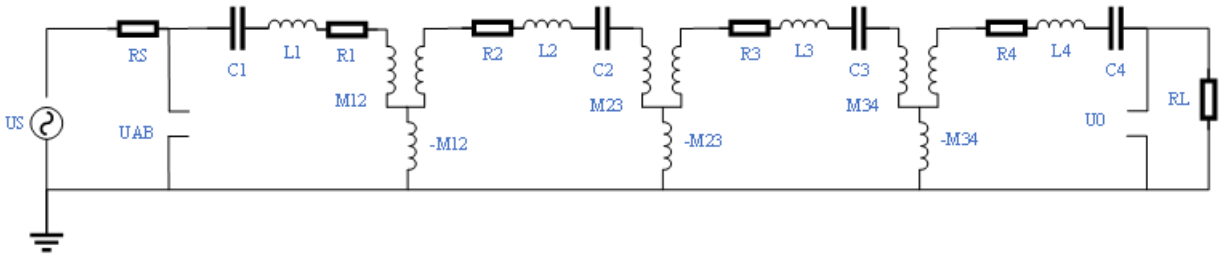

Figure 1: Equivalent circuit diagram of four-coil MRC-WPT system

Figure 1 shows that the voltage of RFPA acting on the driving coil compensating network is U_S. The matching resistance connected in series to the driving coil is R_S, the voltage acting on the driving coil is U_{AB}, the inductance of the driving coil is L_1, the compensation capacitance is C_1, and the internal resistance of the coil is R_1. The inductance of the transmitting relay coil is L_2, the stray capacitance of the coil is C_2, and the internal resistance of the coil is R_2. The inductance of the receiving relay coil is L_3, the stray capacitance of the coil is C_3, and the internal resistance of the coil is R_3. The inductance of the load coil is L_4, the compensation capacitance is C_4, and the internal resistance of the coil is R_4. The driving coil, transmitting relay coil, receiving relay coil and load coil are recorded as coils 1, 2, 3 and 4, respectively.

Forest Chemicals Review
www.forestchemicalsreview.com
ISSN: 1520-0191
March-April 2022 Page No. 877-894
Article History: Received: 08 February 2022, Revised: 10 March 2022, Accepted: 02 April 2022, Publication: 30 April 2022

There is a coupling relationship between each two coils. The coupling coefficients shown in Figure 1 are k_{12}, k_{23}, k_{34}, k_{13}, k_{24}, and k_{14}. Due to the large spacing between coils, the coupling coefficient between coils will be quite small. In the analysis, to simplify the model's difficulty, the influence of k_{13}, k_{24} and k_{14} on the system is generally not considered, and only the coupling coefficients k_{12}, k_{23} and k_{34} between adjacent coils are considered. Mutual inductance between coils is M_{12}, M_{23} and M_{34}, respectively. Equation (6) is to establish the equivalent circuit model of four-coil wireless transmission:

$$\begin{bmatrix} Z_1 & j\omega M_{12} & 0 & 0 \\ j\omega M_{12} & Z_2 & -j\omega M_{23} & 0 \\ 0 & -j\omega M_{23} & Z_3 & j\omega M_{34} \\ 0 & 0 & j\omega M_{34} & R_L+Z_4 \end{bmatrix} \begin{bmatrix} I_1 \\ I_2 \\ I_3 \\ I_4 \end{bmatrix} = \begin{bmatrix} U_{AB} \\ 0 \\ 0 \\ 0 \end{bmatrix} \tag{6}$$

In (6), Z_1 to Z_4 are the equivalent impedance of each coil, $M_{12}=k_{12}\sqrt{L_1L_2}$, $M_{23}=k_{23}\sqrt{L_2L_3}$ and $M_{34}=k_{34}\sqrt{L_3L_4}$. Therefore, equation (6) is simplified to obtain the voltage U_{AB} expression, as shown in (7):

$$U_{AB}=\left(R_1+j\omega L_1+\frac{1}{j\omega C_1}\right) I_1+j\omega M_{12} I_2 \tag{7}$$

The transfer function G between the input side voltage U_{AB} and the output side voltage U_0 is obtained from equation (7), as shown in equation (8):

$$G=\frac{U_o}{U_{AB}}=\frac{R_L I_4}{R_{eq1} I_1} \tag{8}$$

R_{eq1} to R_{eq4} are set as the equivalent resistance from the system input side to each stage coil respectively. Equation (9) is the value from R_{eq1} to R_{eq4}:

$$\begin{cases} \&R_{eq1}=Z_1+R_{eq2} \\ \&R_{eq2}=\dfrac{j\omega M_{12} I_2}{I_1}=\dfrac{-\omega^2 M_{12}^2}{-Z_2+R_{eq3}} \\ \&R_{eq3}=\dfrac{j\omega M_{23} I_3}{I_2}=\dfrac{-\omega^2 M_{23}^2}{Z_3+R_{eq4}} \\ \&R_{eq4}=\dfrac{j\omega M_{34} I_4}{I_3}=\dfrac{\omega^2 M_{34}^2}{Z_4} \end{cases} \tag{9}$$

In order to make the resonant system work normally, compensation capacitors C1-C4 need to be set to meet $L_1C_1=1/\omega_0^2$, $L_2C_2=1/\omega_0^2$, $L_3C_3=1/\omega_0^2$, and $L_4C_4=1/\omega_0^2$. Moreover, the stray capacitance of the coil needs to adjust the shape, size and line spacing of the coil to meet the conditions of system resonance. Among them, ω_0 is the natural resonance frequency of the relay coil. In the case of resonance between coils, the transfer function equation of the input power supply U_S and the load output voltage U_0 of the four-coil MRC-WPT system is as follows.

Forest Chemicals Review
www.forestchemicalsreview.com
ISSN: 1520-0191
March-April 2022 Page No. 877-894
Article History: Received: 08 February 2022, Revised: 10 March 2022, Accepted: 02 April 2022, Publication: 30 April 2022

$$G_{SSSS}=\frac{-j\omega^3 M_{12}M_{23}M_{34}R_L}{a_1\omega^4+a_2\omega^2+(Z_1+R_s)Z_2Z_3Z_4} \tag{10}$$

In (10), R_s is the input resistance of the series circuit. $a_1=M_{12}^2M_{34}^2$ and $a_2=M_{12}Z_3Z_4+(Z_1+R_s)M_{23}Z_4+(Z_1+R_s)Z_2M_{34}$. Equation (11) is to obtain the overall equivalent input resistance on the input side:

$$Z_{in\_-SSSS}=R_s+R_{eq1}=\frac{a_1\omega^4+a_2\omega^2+(R_s+Z_1)Z_2Z_3Z_4}{\omega^2Z_2M_{34}+\omega^2M_{23}Z_4+Z_2Z_3Z_4} \tag{11}$$

Equation (12) is the expression of the overall transmission efficiency of the wireless transmission system under the compensating network:

$$\eta_{T\_SSSS}=\frac{P_O}{P_s}=\frac{-\omega^6M_{12}{}^2M_{23}{}^2M_{34}{}^2R_L}{[Z_4(Z_2Z_3+\omega^2M_{23}{}^2)+\omega^2M_{34}{}^2Z_2]^2(R_s+R_{eq1})} \tag{12}$$

Equation (13) displays the expression of output power.

$$P_{O\_SSSS}=\frac{U_O^2}{R_L} \tag{13}$$

2.3 Analysis of LCC-SSS compensating network

The traditional SSSS compensating network has matching resistance, so the wireless transmission system is difficult to meet the power requirements. The traditional low-order compensation has the problems that the circuit sensitivity of the resonant element is too high and the input-output gain is not adjustable. Moreover, the SSSS compensating network can reveal that the input equivalent resistance presents an inductive region, resulting in large input reactive power, affecting system efficiency [19-21]. This exploration is based on the commonly used high-order compensating network to design the input impedance of the system to solve these problems. Since the compensating network of the relay coil cannot be changed into a high-order compensating network by increasing the compensation capacitance or inductance, the compensator can be designed for the driving coil on the input side or the load coil on the output side. The driving coil compensation topology is set as an LCC compensating network.

Under steady-state conditions, the LCC network circuit can adjust the current on the transmitting coil by reasonably selecting the capacitance value in series. Meanwhile, it can isolate the DC component on the power side and avoid the DC magnetization of the transmission coil. The overall structure of the system is the compensating network of LCC-SSS. The high-order compensator is used as the resonant network of the driving coil, which can make the input impedance of the system zero to improve the transmission efficiency of the system [22-24].

The LCC network consists of L_0, C_0, L_1 and C_1 to form a resonant cavity. R_0 is the parasitic resistance of the LCC network. The output current I_0 of U_S matches the impedance of the driving coil through the

Forest Chemicals Review
www.forestchemicalsreview.com
ISSN: 1520-0191
March-April 2022 Page No. 877-894
Article History: Received: 08 February 2022, Revised: 10 March 2022, Accepted: 02 April 2022, Publication: 30 April 2022

LCC compensating network. Primary side controlled source $j\omega M_{12}I_{12}$ is equivalent to pure resistance R_{eq2}, so the LCC network on the primary side of the driving coil can be analyzed. According to the analysis of the purely resistive second-order resonant network, the primary side compensating inductance L_0 and its corresponding compensation capacitance C_0 should meet $j\omega_0 L_0=\frac{\cdot}{j\omega_0 C_1}+j\omega_0 L_1$ to realize the zero phase angle (ZPA) input of the system.

Figure 2 reveals the equivalent circuit of LCC-SSS compensating network of four-coil MRC-WPT wireless transmission system:

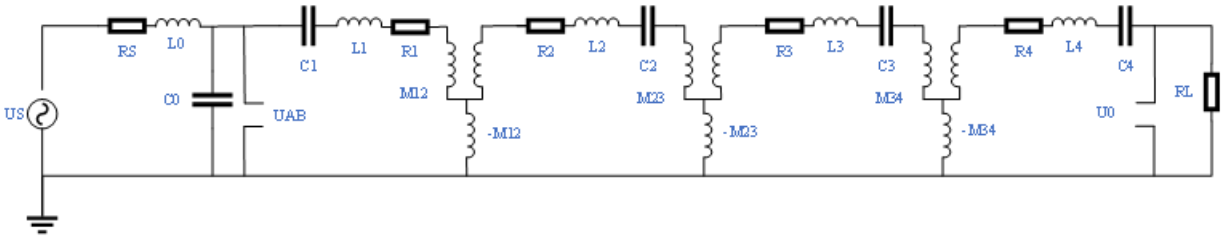

Figure 2: the equivalent circuit of LCC-SSS compensating network of four-coil MRC-WPT wireless transmission system

The resonance condition of the LCC-SSS compensating network shall meet equation (14) to meet the working conditions of the system:

$$\begin{cases} L_0C_0=1/\omega_0^2 \\ (L_1-L_0)C_1=1/\omega_0^2 \\ L_2C_2=1/\omega_0^2 \\ L_3C_3=1/\omega_0^2 \\ L_4C_4=1/\omega_0^2 \end{cases} \tag{14}$$

For the LCC network, the transfer function of output voltage U_{AB} and input voltage U_S is $G_{LCC}=\frac{U_{AB}}{U_S}=\frac{R_{eq1}}{(R_0+j\omega L_0)(1+j\omega C_0 R_{eq1})+R_{eq1}}$.

Equation (15) and equation (16) are the transfer function and equivalent input impedance of LCC-SSS compensated four-coil wireless transmission system respectively:

$$G_{LCC\text{-}SSS}=G\cdot G_{LCC} \tag{15}$$

$$Z_{in\_LCC\text{-}SSS}=R_0+j\omega L_0+\frac{R_{eq1}}{1+j\omega C_0 R_{eq1}} \tag{16}$$

According to the transfer function G_{LCC}, the transmission efficiency of the system is obtained as shown in equation (17):

Forest Chemicals Review
www.forestchemicalsreview.com
ISSN: 1520-0191
March-April 2022 Page No. 877-894
Article History: Received: 08 February 2022, Revised: 10 March 2022, Accepted: 02 April 2022, Publication: 30 April 2022

$$\eta_{T\_LCC\text{-}SSS}=\frac{R_L I_4{}^2}{\left(R_0+j\omega L_0+\frac{R_{eq1}}{1+j\omega C_0 R_{eq1}}\right)\left(j\omega C_0\cdot R_{eq1}\right)^2 I_1^2} \tag{17}$$

In (17), the value of I_4/I_1 is $\frac{-j\omega^3 M_{12}M_{23}M_{34}}{Z_4\left(Z_2Z_3+\omega^2M_{23}^2\right)+\omega^2M_{34}^2Z_2}$.

α is defined as the inductance coefficient between L_0 and L_1, and the value range is (0,1). Then, equation (18) is the expression of the transfer function $G_{LCC\text{-}SSS}$ of LCC-SSS system about α:

$$G_{LCC\text{-}SSS}=\frac{G\cdot R_{eq1}}{\left(R_0+j\omega\alpha L_1\right)\left(1+j\omega\frac{1-\alpha}{\alpha}C_1R_{eq1}\right)+R_{eq1}} \tag{18}$$

Equation (19) is the expression of input impedance $Z_{in\_LCC\text{-}SSS}$ of LCC-SSS system about α:

$$Z_{in\_LCC\text{-}SSS}=R_0+j\omega\alpha L_1+\frac{\alpha R_{eq1}}{\alpha+(1-\alpha)j\omega C_1R_{eq1}} \tag{19}$$

Equation (20) is the expression of transmission efficiency $\eta_{T\_LCC\text{-}SSS}$ of LCC-SSS system about α:

$$\eta_{T\_LCC\text{-}SSS}=\frac{R_L I_4{}^2}{\left(R_0+j\omega\alpha L_1+\frac{\alpha R_{eq1}}{\alpha+j\omega(1-\alpha)C_1R_{eq1}}\right)\left(j\omega\frac{1-\alpha}{\alpha}C_1R_{eq1}\right)^2 I_1^2} \tag{20}$$

The value of system output power $P_{O\_LCC\text{-}SSS}$ during LCC-SSS compensating network is $\frac{U_O{}^2}{R_L}$.

III. EXPERIMENTAL VERIFICATION AND ANALYSIS

3.1 Experimental verification of different compensating networks

For the traditional SSSS compensating network, the series matching resistance usually affects the transmission gain of the system. The series matching resistance R_S is set to 0 and the output resistance R_L is set to 50Ω. It is stimulated when the coupling coefficient k_{23} is equal to 0.001, 0.01, 0.1 and 0.5, respectively. Figure 3 and Figure 4 are the obtained curves of the transmission gain and input current gain of the system with or without input series matching resistance:

Forest Chemicals Review
www.forestchemicalsreview.com
ISSN: 1520-0191
March-April 2022 Page No. 877-894
Article History: Received: 08 February 2022, Revised: 10 March 2022, Accepted: 02 April 2022, Publication: 30 April 2022

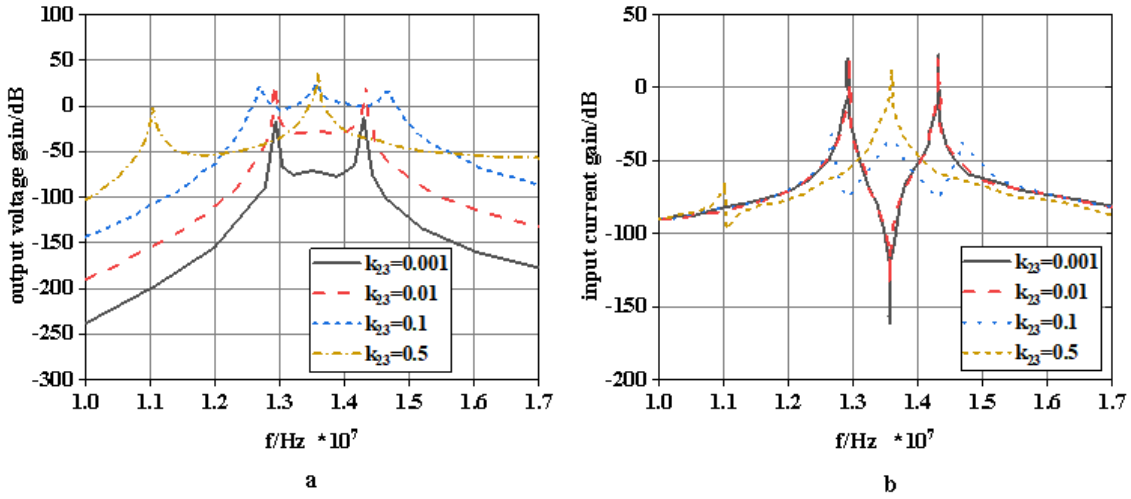

Figure 3: system output voltage gain and input current gain without series matching resistance (a is input voltage gain and b is input current gain.)

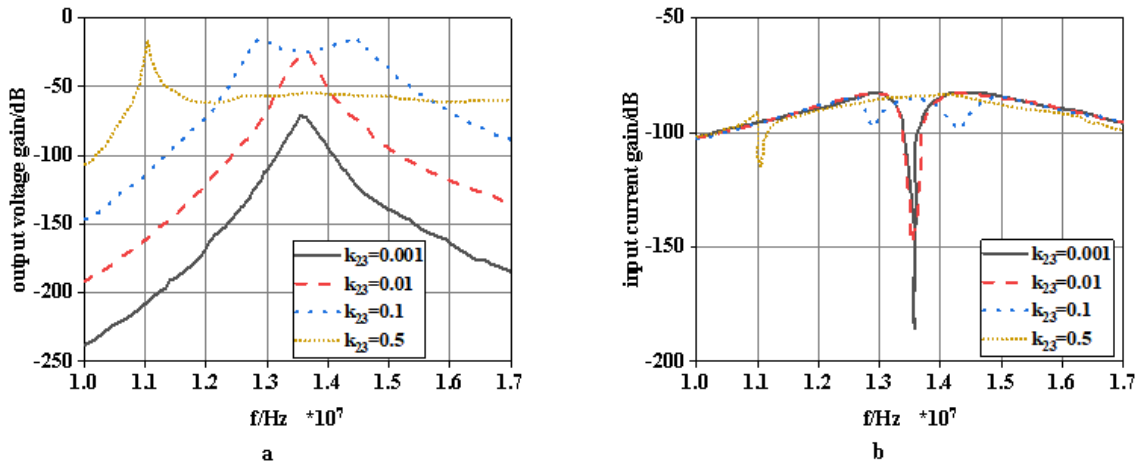

Figure 4: output voltage gain and input current gain of the system when 50Ω matching resistor is connected in series (a is the input voltage gain and b is the input current gain.)

Figure 3 reveals that the output voltage gain of the system is large when the series matching resistance is 0, because there is no matching resistance, resulting in a relatively high voltage acting on the driving coil. The current gain at the input side of the system is also large, up to 24dB. Due to the surge of input current, circuit components may be damaged, and the system's normal operation cannot be guaranteed.

Figure 4 shows that the voltage output gain of the system has obvious frequency splitting when adding 50Ω matching resistance. The maximum output voltage of the whole system does not exceed -14dB, and the gain of the input current is also small, resulting in small transmission power and efficiency of the whole system, which will limit the output power in the actual system.

Forest Chemicals Review
www.forestchemicalsreview.com
ISSN: 1520-0191
March-April 2022 Page No. 877-894
Article History: Received: 08 February 2022, Revised: 10 March 2022, Accepted: 02 April 2022, Publication: 30 April 2022

For LCC-SSS compensating network, the parameters L_0 and C_0 on the primary side can be changed by setting α to change the transmission characteristics of the system. In the actual system, L_0 and C_0 are generally fixed values, so it is necessary to consider the overall transmission characteristics to determine an optimal α, so that the system can still obtain high output power and transmission efficiency at different k_{23}. The values of α are set to 0.2, 0.4, 0.6 and 0.8, respectively for curve drawing and simulation analysis. Figure 5 shows the transmission characteristics of the LCC compensating network:

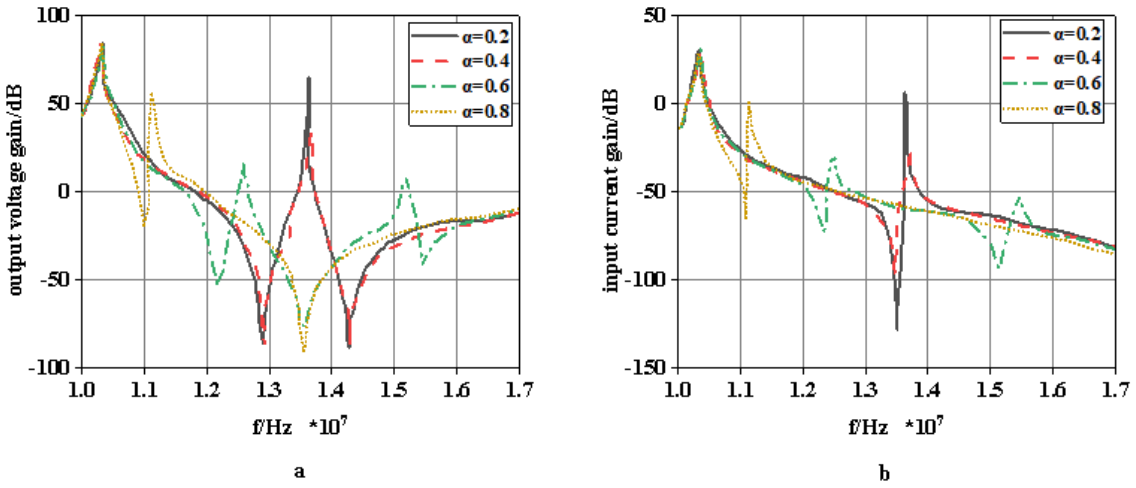

Figure 5: transmission characteristics of LCC compensating network (a is the input voltage gain and b is the input current gain.)

Figure 5 shows that when α is smaller, the gain of the input current at the resonant frequency is higher, while when α is larger, the gain at the resonant frequency is smaller. It is equivalent to that the LCC compensating network controls the overall input current and reduces the voltage acting on the inductance of the driving coil to control the power of the whole system.

The inductance coefficient determines the output power and transmission efficiency of the actual system, so the influence of different inductance coefficients on the system characteristics is quite different. The curve in Figure 6 is drawn according to the equation of output power and transmission efficiency to select a reasonable inductance coefficient α:

Forest Chemicals Review
www.forestchemicalsreview.com
ISSN: 1520-0191
March-April 2022 Page No. 877-894
Article History: Received: 08 February 2022, Revised: 10 March 2022, Accepted: 02 April 2022, Publication: 30 April 2022

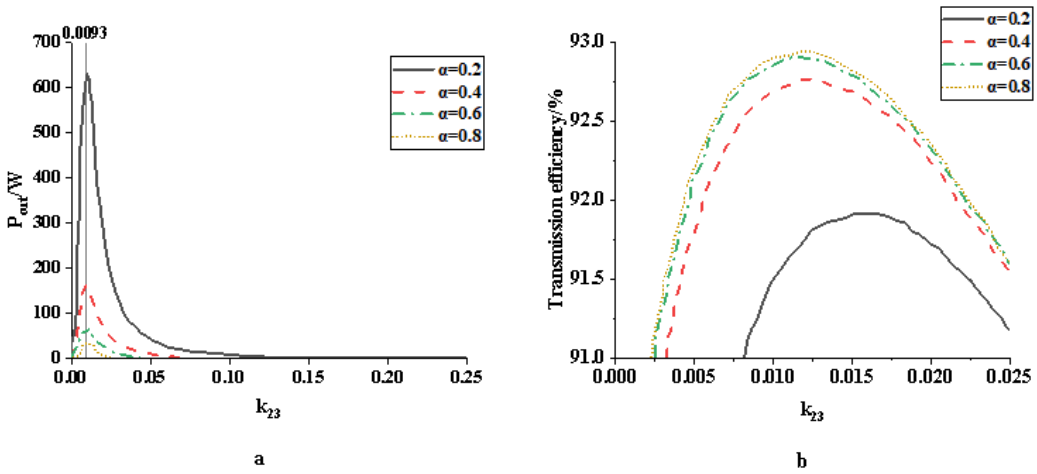

Figure 6: variation of system output power and transmission efficiency with coupling coefficient k_{23} under different inductance coefficients (a is output power, and b is transmission efficiency)

Figure 6a is a curve showing the change of system output power caused by the change of k_{23} when values of α are selected. The output power shows that when α is smaller, the maximum output power is larger. Moreover, no matter what α is, the corresponding k_{23}=0.0093 when the output power reaches the maximum value. It shows that in the LCC-SSS compensating network, the system's output power reaches the maximum at a fixed coupling coefficient k_{23}, and the corresponding transmission distance at the maximum power does not change with α.

Figure 6b is a curve showing the change of system transmission efficiency caused by the change of k_{23} when values of α are selected. It reveals that when α is smaller, the overall transmission efficiency of the system is smaller. The smaller the α is, the greater the current on the input side is. At this time, the greater the energy loss on the internal resistance and parasitic parameters of each coil is, the smaller the transmission efficiency of the system is. The curve suggests that when α is smaller, the k_{23} at the maximum transmission efficiency of the system is smaller, which shows that the system can achieve more efficient energy transmission at a longer transmission distance.

Figure 7 is the curve of the output voltage gain and input current gain of the system at different transmission distances, that is, different coupling coefficients:

Forest Chemicals Review
www.forestchemicalsreview.com
ISSN: 1520-0191
March-April 2022 Page No. 877-894
Article History: Received: 08 February 2022, Revised: 10 March 2022, Accepted: 02 April 2022, Publication: 30 April 2022

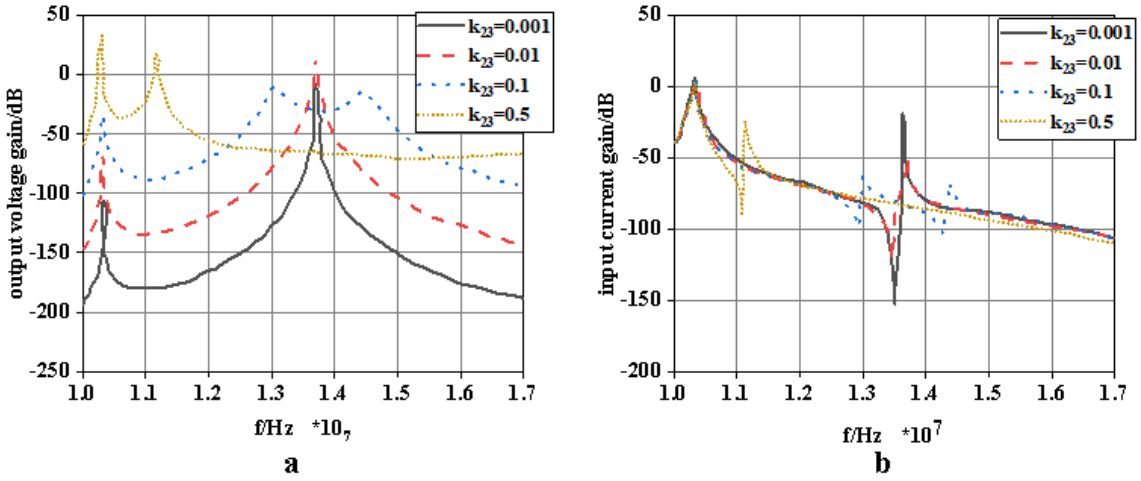

Figure 7: system output voltage gain and input current gain when inductance coefficient α is 0.6 (a is the input voltage gain and B is the input current gain.)

Figure 7 shows that using LCC-SSS compensating network can solve the problem of small output current gain of SSSS compensating network when R_S=0. Compared with the SSSS network, the LCC-SSS compensating network can simultaneously meet the maximum output power and transmission efficiency.

3.2 Analysis of experimental verification results

The system cannot work normally when the traditional SSSS compensating network has no series compensation resistance, so the experiment is only carried out for the SSSS compensating network when R_S=R_L. During the experiment, all coils are on the same line, only the distance between relay coils is changed, and the input voltage at the DC side is changed to make the voltage at both ends of the driving coil 50V. Table 1 shows the experimental data of the SSSS compensating network:

TABLE 1: Experimental data of SSSS compensating network

k_{23}	d_{23}	U_{DC}	U_S	U_0
0.001	31	51	50.75	0.77
0.005	20	47	50.5	7.9
0.01	14	46	49.5	17.1
0.1	7	79	49.5	4.5

The value of the inductance coefficient α for the LCC-SSS compensating network is 0.6. The experimental data are measured when the LCC compensating network is applied to the driving coil. Table 2 shows the experimental data:

TABLE 2: Experimental data of the LCC-SSS compensating network

k_{23}	d_{23}	U_{DC}	U_S	U_0

Forest Chemicals Review
www.forestchemicalsreview.com
ISSN: 1520-0191
March-April 2022 Page No. 877-894
Article History: Received: 08 February 2022, Revised: 10 March 2022, Accepted: 02 April 2022, Publication: 30 April 2022

0.001	31	13	48.75	2.3
0.005	20	17	48.5	13.9
0.01	14	41	49.5	28.9
0.1	7	178	49.5	19.9

The measured coil spacing is converted into a coupling coefficient, and the input voltage of the driving coil and the output voltage of the load coil are recorded. The output power and transmission efficiency are calculated. Figure 8 is the variation curve when the coupling coefficient is 0-0.3:

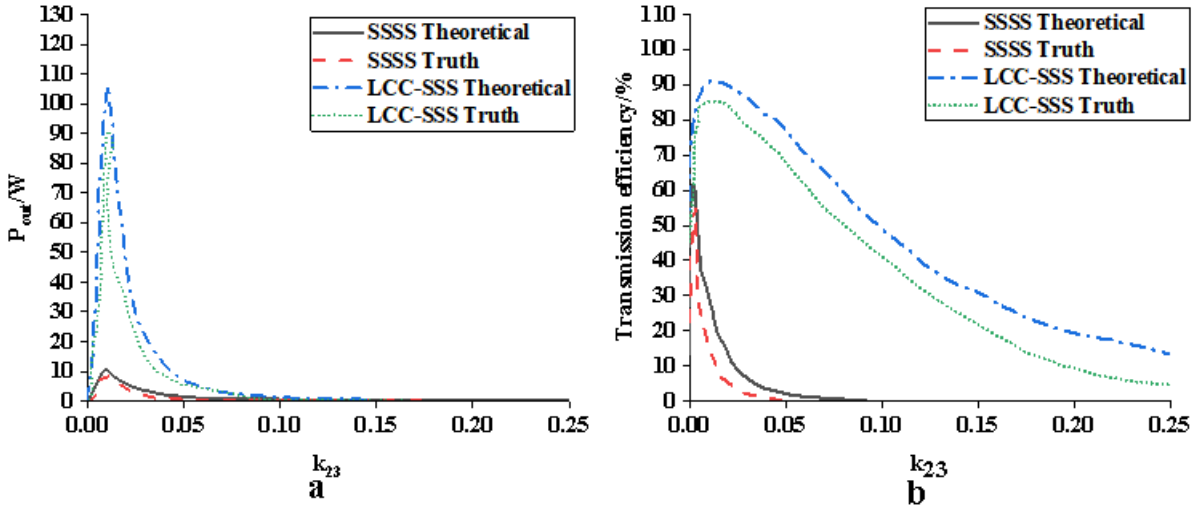

Figure 8: experimental curves of output power and transmission efficiency of the system in different compensating networks (a is output power and b is transmission efficiency)

Figure 8a shows that when the distance between the relay coils of the four-coil MRC-WPT system is from far to near, the coupling coefficient of the system is too small due to the too far distance between the coils. Hence, the influence component of the coupling coefficient on the system is small, resulting in the relatively small transmission power of the system. However, as the distance gets closer, the influence of the coupling coefficient on the system increases. Moreover, when the system approaches the optimal transmission distance, the system's output power reaches the maximum. With the further reduction of transmission distance, the frequency splitting of the system caused by too large coupling coefficient becomes increasingly serious. It makes the system deviate from the optimal resonant frequency, the output voltage of the system decrease significantly, and the output power also decrease. SSSS compensating network introduces series matching resistance R_S. The existence of series matching resistance will reduce the input current of the system and the power acting on the system. Moreover, the existence of R_S makes the energy dissipated as heat energy, resulting in a significant increase in the unnecessary energy consumption of the system. For LCC-SSS compensating network, there are no energy-consuming components in the system. Through the combination of passive components, the energy in the system is stored in the resonant element without input series resistance, which increases the voltage acting on the driving coil, increases the input current flowing through the system, and improves the output power of the system. Under the same conditions, when the inductance coefficient is 0.5, the maximum output power of

Forest Chemicals Review
www.forestchemicalsreview.com
ISSN: 1520-0191
March-April 2022 Page No. 877-894
Article History: Received: 08 February 2022, Revised: 10 March 2022, Accepted: 02 April 2022, Publication: 30 April 2022

the LCC-SSS compensating network can reach 85W, while that of the SSSS compensating network is only 10W. However, both compensation networks reach the system's maximum power at the same coupling coefficient.

Figure 8b shows that when the distance between the relay coils of the four-coil MRC-WPT system is from far to near, the transmission efficiency of the system is also quite low when the distance is far. This is because the distance between the coils is too far and the coupling coefficient between the coils is too small, which will reduce the energy transmitted between the coils, resulting in the low transmission efficiency of the system. As the distance decreases, the input voltage, input current and output voltage of the system increase simultaneously, and the coupling coefficient of the system will lead to appropriate resonance between coils. At this time, the transmission efficiency of the system also increases. However, with the further reduction of the distance between coils, the transmission efficiency of the system will also decrease significantly with the frequency splitting phenomenon of the system.

The same method is used for the LCC-SSS compensating network to measure and record the data of system output power and transmission efficiency under different inductance coefficients. Figure 9 is a curve drawn when the inductance coefficient is 0.2, 0.5 and 0.8, respectively.

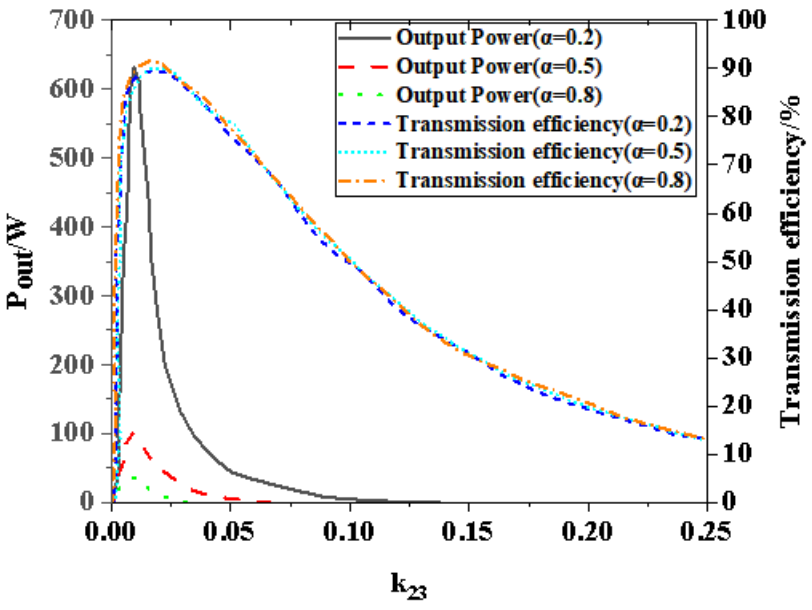

Figure 9: experimental curves of output power and transmission efficiency of the system at different inductance coefficients

Figure 9 shows that when the inductance coefficient α is changed, the overall transmission efficiency of the system basically does not change. This is due to the resonant charge and discharge when the passive device is introduced to work, and the passive device does not lose energy with heat energy. Therefore, the

Forest Chemicals Review
www.forestchemicalsreview.com
ISSN: 1520-0191
March-April 2022 Page No. 877-894
Article History: Received: 08 February 2022, Revised: 10 March 2022, Accepted: 02 April 2022, Publication: 30 April 2022

introduction of passive devices generally has no impact on the transmission efficiency of the system. When the actual MRC-WPT system works, the reduction of α will make the overall working current of the system too large and produce a certain energy loss. However, the losses are acceptable, and the overall transmission efficiency of the system is much higher than that of the SSSS compensating network.

At present, the research on MRC-WPT with a four-coil structure is more about the analysis and interpretation of the circuit and how to improve the system's transmission distance and transmission efficiency. The analysis of the input matching resistance of the system is relatively few. Generally, when the system works, it often needs input series resistance to realize the impedance matching of the RF power operational amplifier circuit. Typically, 50Ω, 25Ω or 75Ω are used. In the analysis, the power loss on the matching resistance is often ignored, and only the coil structure's transmission efficiency and output power are analyzed. The existence of matching resistance greatly reduces the overall transmission efficiency of the system, which is relatively less studied at present. In the analysis process, this thesis mainly studies the influence of system matching resistance and establishes the mathematical model of the relationship between matching resistance and system transmission efficiency and output power. The analysis results show that the matching resistance will always have an adverse impact on the system. Therefore, this thesis is mainly to analyze the processing mode of matching resistance and the selection of matching circuits to make the system better transmit energy and improve the overall transmission efficiency of the system.

IV. Conclusion

This thesis is to improve the charging distance and charging efficiency of electric vehicles. Electric vehicles' wireless charging control strategy based on compensation networks is mainly studied. First, with the four-coil MRC-WPT system as the research object, the working principle of the circuit is analyzed, and the influence of the series matching resistance of the traditional SSSS compensation network on the transmission gain of the system is discussed. Then, an LCC-SSS compensation network applied to a four-coil MRC-WPT system is proposed and analyzed. Finally, through theoretical analysis and experiments, the transmission distance and output voltage on the load when the system works in different compensation networks are measured, and the variation curves of the output power and transmission efficiency of the system are drawn. The curves of output power and transmission efficiency when the LCC-SSS compensation network selects different inductance coefficients are analyzed, and the selection range of inductance coefficients is obtained. The experimental results show that there are no energy-consuming components in the wireless charging system based on LCC-SSS compensation network. Through the combination of passive devices, the energy in the system is stored in the resonant element without input series resistance, which increases the voltage acting on the driving coil, increases the input current flowing through the system, and improves the output power of the system. It is proved that the proposed LCC-SSS compensation network effectively improves the system's output power and transmission efficiency. Due to limited energy, the coupling relationship between non-adjacent coils has not been considered in this analysis. Further research will be carried out in the future, and more types of compensation networks will be applied to the wireless transmission system with a four-coil structure. This thesis has certain reference significance for the compensation network optimization of electric vehicle wireless charging systems.

Forest Chemicals Review
www.forestchemicalsreview.com
ISSN: 1520-0191
March-April 2022 Page No. 877-894
Article History: Received: 08 February 2022, Revised: 10 March 2022, Accepted: 02 April 2022, Publication: 30 April 2022

REFERENCES

1. Tian, J., Xiong, R., Shen, W., Lu, J. (2021). State-of-charge estimation of lifepo4 batteries in electric vehicles: a deep-learning enabled approach. Applied Energy, 291(3), 116812.
2. Curtale, R., Liao, F., Waerden, P. (2021). Understanding travel preferences for user-based relocation strategies of one-way electric car-sharing services. Transportation Research Part C Emerging Technologies, 127(3), 103135.
3. Jin, K., Zhou, W. (2019). Wireless Laser Power Transmission: A Review of Recent Progress. IEEE Transactions on Power Electronics, 34(4), 3842-3859.
4. Xu, J., Dai, F., Xu, Y., Li, C. (2019). Wireless power supply technology for uniform magnetic field of intelligent greenhouse sensors. Computers and Electronics in Agriculture, 156, 203-208.
5. Zhang, Z., Chen, C., Fei, T., Xiao, H., Xie, G., Cheng, X. (2019). Wireless communication and wireless power transfer system for implantable medical device. Journal of Semiconductors, 41(10), 7.
6. Seo, D. W. (2019). Comparative Analysis of Two- and Three-Coil WPT Systems Based on Transmission Efficiency. IEEE Access, 7, 151962-151970.
7. Liao, Z., Sun, Y., Ye, Z., Tang, C. and Wang, P. (2019). Resonant Analysis of Magnetic Coupling Wireless Power Transfer Systems. IEEE Transactions on Power Electronics, 34(6), 5513-5523
8. Dai, Z., Wang, J., Zhou, H., Huang, H. (2020). A Review on the Recent Development in the Design and Optimization of Magnetic Coupling Mechanism of Wireless Power Transmission. IEEE Systems Journal, 99, 1-14.
9. Tomura, T., Hirokawa, J., Furukawa, M., Fujiwara, T., Shinohara, N. (2021). Eight-Port Feed Radial Line Slot Antenna for Wireless Power Transmission. IEEE Open Journal of Antennas and Propagation, 2, 170-180.
10. Srivani, S. G., Gagana, P. (2019). Wireless Power Transmission via Solar Power Satellite. Electrical India, 59(7), 72-74, 76-77.
11. Miura, D., Tokudaiji, Y., Murasato, K., Hattori, Y., Bu, Y., Mizuno, T. (2019). Investigation of Structure and Material for Back Yoke at 13.56 MHz Wireless Power Transfer Focused on High Transmission Efficiency. IEEE Transactions on Magnetics, 7,1-5.
12. Li, Y., Wei, Y., Wang, Q., Huang, Y., Cheng, J. (2019). Design Method of High Efficiency Class-E Inverter Applied to Magnetic Coupled Resonant Wireless Power Transmission System. Diangong Jishu Xuebao/Transactions of China Electrotechnical Society, 34(2), 219-225.
13. Peng, Y., Saito, K., Ito, K. (2019). Dual-Band Antenna Design for Wireless Capsule Endoscopic Image Transmission in the MHz Band Based on Impulse Radio Technology. IEEE Journal of Electromagnetics, RF and Microwaves in Medicine and Biology, 3(3), 158-164.
14. Hua, M., Wang, Y., Wu, Q., Dai, H., Yang, L. (2019). Energy-Efficient Cooperative Secure Transmission in Multi-UAV Enabled Wireless Networks. IEEE Transactions on Vehicular Technology, 68(8), 7761-7775.
15. Choi, H. S., Choi, S. J. (2019). Compact Drive Circuit for Capacitive Wireless Power Transfer System Utilizing Leakage-Enhanced Transformer. Journal of Electrical Engineering & Technology, 14(1), 1-9.

Forest Chemicals Review
www.forestchemicalsreview.com
ISSN: 1520-0191
March-April 2022 Page No. 877-894
Article History: Received: 08 February 2022, Revised: 10 March 2022, Accepted: 02 April 2022, Publication: 30 April 2022

16. Mamaghani, M. T., Abbas, R. (2019). Security and reliability performance analysis for two-way wireless energy harvesting based untrusted relaying with cooperative jamming. Communications, IET, 13(4), 449-459.
17. Fan, X., He, J., Mu, J., Qian, J., Chou, X. (2019). Triboelectric-Electromagnetic Hybrid Nanogenerator Driven by Wind for Self-powered Wireless Transmission in Internet of Things and Self-Powered Wind Speed Sensor. Nano Energy, 68, 104319.
18. Yu, Z., Chi, K., Hu, P., Zhu, Y. H., & Liu, X. (2019). Energy Provision Minimization in Wireless Powered Communication Networks With Node Throughput Requirement. IEEE Transactions on Vehicular Technology, 68(7), 7057-7070.
19. Wang, X., Zhu, X. W., Tian, L., Liu, P., Hong, W., Zhu, A. (2019). Design and Experiment of Filtering Power Divider Based on Shielded HMSIW/QMSIW Technology for 5G Wireless Applications. IEEE Access, 7, 72411-72419.
20. Huang, Y., Zhao, J., Sun, W., Yang, H., Liu, Y. (2019). Investigation and Modeling of Multi-Node Body Channel Wireless Power Transfer. Sensors, 20(1), 156.
21. Lim, T., Kim, Y. (2019). Compact Self-Powered Wireless Sensors for Real-Time Monitoring of Power Lines. Journal of Electrical Engineering and Technology, 14(3), 1321-1326.
22. Choudhary, A., Nizamuddin, M., Singh, M. K., Sachan, V. K. (2019). Energy Budget Based Multiple Attribute Decision Making (EB-MADM) Algorithm for Cooperative Clustering in Wireless Body Area Networks. Journal of Electrical Engineering and Technology, 14(1), 421-433.
23. Kim, W., Ahn, D. (2019). Efficient deactivation of unused LCC inverter for multiple transmitter wireless power transfer. IET Power Electronics, 12(1), 72-82.
24. An, H., Liu, G., Li, Y., Song, J., Liu, M. (2019). Inhomogeneous electromagnetic metamaterial design method for improving efficiency and range of wireless power transfer. IET Microwaves, Antennas & Propagation, 13(12), 2110-2118.